EARTHQUAKE ENGINEERING AND STRUCTURAL DYNAMICS, VOL. 26, 549–570 (1997)

EFFECTIVE OPTIMAL STRUCTURAL CONTROL OF SOIL–STRUCTURE INTERACTION SYSTEMS

H. ALLISON SMITH*

Department of Civil Engineering, Stanford University, Stanford, California 94305-4020, U.S.A.

AND

WEN-HWA WU†

Department of Construction Engineering, National Yunlin Institute of Technology, Yunlin, Taiwan 640, Republic of China

SUMMARY

A methodology is developed in this paper to include soil–structure interaction effects in optimal structural control, General Multi-Degree-Of-Freedom (MDOF) structural models are considered. The SSI transfer functions for ground motion and control force in the physical space are presented first, followed by a methodology for using system identification techniques to find an equivalent fixed-base model of an MDOF SSI system. An iterative technique is applied to combine these methods for the determination of optimal control gains. The control effectiveness of considering soil–structure interaction is investigated for the controlled SSI system. It is found that the control algorithm considering SSI effects is more effective than the corresponding control algorithm assuming a fixed-base system model. In addition, the advantage of applying this methodology is observed to be more prominent in the cases where the SSI effects are more significant. © 1997 by John Wiley & Sons, Ltd.

KEY WORDS: structural control; earthquake engineering; soil–structure interaction; structural dynamics

1. INTRODUCTION

It has been generally recognized that Soil–Structure Interaction (SSI) can drastically affect the responses of structures subjected to earthquake excitations. Therefore, the inclusion of SSI effects is particularly important in the analysis of structures located in active seismic zones. However, in the majority of the research devoted to active structural control, the structural models utilized are highly simplified fixed-base systems. Only recently has soil–structure interaction been included in the control problem.[1–4]

To consider SSI effects in structural control, the analysis is extended from the structural model to include the total structure–foundation–soil system, which involves an infinite half-space. The substructure method is commonly adopted in the SSI analysis where a mixed boundary-value problem in elastodynamics is first solved to obtain the foundation impedances of soils and then utilized to analyse the structure–foundation model. Using this method to include SSI effects in a control algorithm, the problem formulation is similar to that of the Control/Structure Interaction (CSI) problem. However, it should be noted that since the foundation impedances are frequency-dependent in the SSI/control problem, the solution techniques used for the CSI problem, where the parameters in actuator dynamics are considered constant, cannot be applied. Therefore, the development of new methodologies is required to solve the SSI/control problem.

The major difficulty in including soil–structure interaction in optimal structural control comes from the fact that analysis of an SSI system is usually formulated in the frequency domain due to the frequency-dependent foundation impedances, whereas the conventional optimal control problem is performed in the

*Assistant Professor
†Associate Professor

CCC 0098–8847/97/050549–22$17·50

Received 15 August 1994
Revised 6 June 1996

time domain. One way to tackle this problem is to integrate the soil–structure interaction force in the time domain using inverse Fourier transform and convolution techniques and then to include it in the control algorithm.[2] However, this method is computationally intensive, which may cause problems in on-line control applications. In addition, the requirement of satisfying the causality condition to avoid the difficulty of knowing the future system response *a priori* limits the use of accurate foundation impedances. An alternative approach is to use approximate frequency-independent values for the foundation impedances and formulate the whole SSI/control problem in the time domain.[3] Even though an observer can be introduced to compensate for the inaccurate representation of SSI effects, the observation spillover due to the uncontrolled modes causes another concern.

Using an equivalent fixed-base structural model to represent the whole SSI system, an effective approach has recently been developed by the authors to include SSI effects in the optimal control algorithms. Smith *et al.*[4,5] studied the formulation of the externally controlled system where the actuator exerts control forces only to the structure and is not connected to the foundation. The SSI/control equations were formulated with the approximation via replacement oscillator to determine the optimal control gains. Wu and Smith[6,7] presented a formulation for the internally controlled system where the exerted control forces are internally reacted between the superstructure and foundation. An iterative algorithm was employed to determine the optimal control gains which are interrelated to the SSI factors in this case. With this proposed method, the control scheme can be implemented in the framework of a conventional optimal control algorithm used for a fixed-base structure such that computational complexity is significantly reduced. The tradeoff is the computational cost associated with *a priori* determination of the equivalent fixed-base structure needed for obtaining the optimal gain factors; however, this is not of primary concern considering the powerful computation ability of modern computers.

This paper extends the above research to consider general Multi-Degree-Of-Freedom (MDOF) structural models. The SSI transfer functions for ground motion and control force in the physical space are presented first, followed by a methodology for using system identification techniques to find an equivalent fixed-base model of an MDOF SSI system. An iterative technique is applied to combine these methods for the determination of optimal control gains. Numerical examples are presented to show that the control algorithm considering SSI effects is more effective than the corresponding control algorithm assuming a fixed-base system model. In addition, the advantage of applying this methodology is observed to be more prominent in the cases where the SSI effects are more significant.

2. SSI TRANSFER FUNCTIONS FOR GROUND MOTION AND CONTROL FORCE

In determining the structural responses of uncontrolled systems, SSI effects can be considered by modifying the translational free-field ground motion that is applied to the structure's foundation. The effects of foundation translation and rotation can be combined such that the SSI effects are quantified through a modification factor, referred to as an SSI transfer function in the frequency domain, operating on the free-field ground motion. In addition to the ground motion, the control force is another external force to the actively controlled system and, thus, requires a corresponding transfer function to account for the SSI effects in the frequency domain. Incorporating the derivation by Prasad[8] for the SSI transfer function for a Single-Degree-Of-Freedom (SDOF) structural model, previous work by the authors has formulated the control equations to consider SSI with the SSI transfer functions for both the ground motion and control force.[4,7]

In a recent paper by the authors,[9] the SSI (matrix) transfer function for the free-field ground motion was derived in the modal space for a general MDOF structural model and applied to compute the structural response. This transfer function is derived here in the physical space to prepare for its application in optimal structural control problems, where the state equation is always expressed in physical variables for practical applications. This section also presents the SSI (matrix) transfer function for the control force of an MDOF structural model for externally and internally controlled systems. An algorithm using the modal superposition method is developed to efficiently compute those SSI transfer functions.

2.1. SSI transfer function for ground motion

The system investigated, shown in Figure 1, is represented by an N-storey shear building resting on a rigid, square foundation of mass m_0 and half side-width b at the surface of a homogeneous elastic half-space. The mass of this building is considered to be concentrated at each floor level and the columns are assumed to have infinite axial rigidity. This representation leads to a system of $(N + 2)$ DOFs: one horizontal translation (relative to the foundation) for each floor, x_j, where $j = 1$–N; the absolute horizontal translation of the foundation, x_0; and the absolute rotation of the system, θ. The mass and height of the jth floor are denoted by m_j and h_j, respectively. Proportional viscous damping is assumed for the structure such that the fixed-base structure possesses classical normal modes. Complete bonding is assumed between the foundation and the supporting soil, which is characterized by its mass density, ρ, shear velocity, v_s, and Poisson's ratio, v.

Since the foundation stiffness and damping are dependent on the frequency of excitation, it is most convenient to formulate the interaction problem in the frequency domain. As shown previously by the authors,[9] the equations of motion for the structure–foundation model illustrated in Figure 1 can be expressed in the frequency domain as

$$(-\omega^2\mathbf{M} + \mathrm{i}\omega\mathbf{C} + \mathbf{K})\mathbf{X}(\omega) - \omega^2\mathbf{M}\mathbf{1}X_0(\omega) - \omega^2\mathbf{M}\mathbf{h}\Theta(\omega) = \mathbf{0} \tag{1}$$

$$-\omega^2\mathbf{1}^{\mathrm{T}}\mathbf{M}\mathbf{X}(\omega) + [K_{\mathrm{V}}(\omega) - \omega^2 m_{\mathrm{T}}]X_0(\omega) + [K_{\mathrm{VM}}(\omega) - \omega^2 d_{\mathrm{T}}]\Theta(\omega) = K_{\mathrm{V}}(\omega)X_{\mathrm{g}}(\omega) \tag{2}$$

$$-\omega^2\mathbf{h}^{\mathrm{T}}\mathbf{M}\mathbf{X}(\omega) + [K_{\mathrm{MV}}(\omega) - \omega^2 d_{\mathrm{T}}]X_0(\omega) + [K_{\mathrm{M}}(\omega) - \omega^2 I_{\mathrm{T}}]\Theta(\omega) = K_{\mathrm{MV}}(\omega)X_{\mathrm{g}}(\omega) \tag{3}$$

where $\mathbf{X}$, X_0, Θ, and X_{g} are the Fourier transforms of $\mathbf{x}$, x_0, θ, and x_{g}, respectively; and $\mathbf{x} = \{x_j\}$ is the vector of structural displacements relative to foundation, x_{g} the free-field ground motion, $\mathbf{M}$ the mass matrix of structure, $\mathbf{C}$ the viscous damping matrix of structure, $\mathbf{K}$ the stiffness matrix of structure, $\mathbf{1}$ the column vector

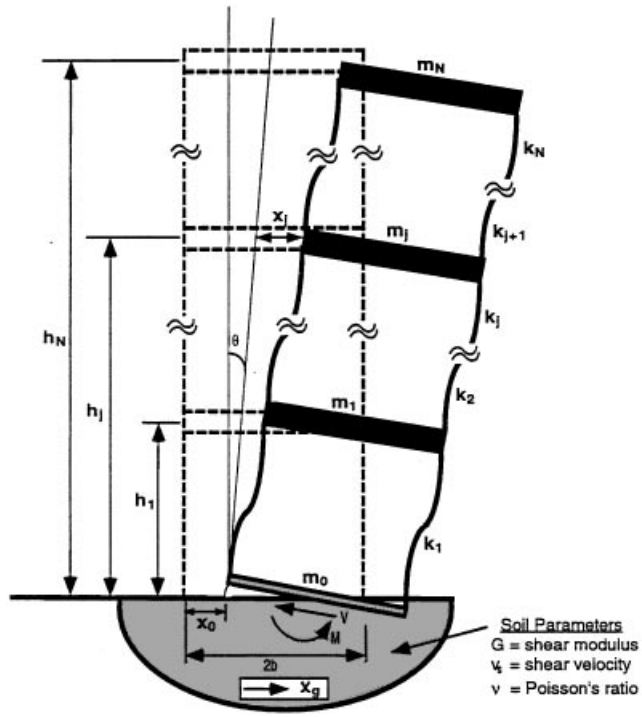

Figure 1. MDOF soil–structure interaction model

where each element is unity, $\mathbf{h} = \{h_j\}$ the column vector of foundation-to-storey heights, $m_T = \sum_{j=0}^{N} m_j$ the total mass of structure and foundation, $d_T = \sum_{j=1}^{N} m_j h_j$, $I_T = I_t + \sum_{j=1}^{N} m_j h_j^2$ the total moment of inertia of structure and footing with respect to the central axis of the footing, K_V the translational impedance of foundation, K_M the rocking impedance of foundation and $K_{VM} = K_{MV}$ (reciprocity theorems) the coupling impedance of foundation.

Defining

$$\mathbf{\Gamma} = \mathbf{M1}, \qquad \mathbf{\Upsilon} = \mathbf{Mh} \tag{4}$$

and the structure transfer function

$$\mathbf{H}(\omega) = -[-\omega^2\mathbf{M} + \mathrm{i}\omega\mathbf{C} + \mathbf{K}]^{-1} \tag{5}$$

the displacement vector can then be solved from equation (1) as

$$\mathbf{X}(\omega) = \omega^2\mathbf{H}(\omega)[X_0(\omega)\mathbf{\Gamma} + \Theta(\omega)\mathbf{\Upsilon}] \tag{6}$$

Applying equation (6), equations (2) and (3) can be rewritten as

$$-\omega^2 \begin{bmatrix} T_V(\omega) & T_{VM}(\omega) \\ T_{MV}(\omega) & T_M(\omega) \end{bmatrix} \begin{Bmatrix} X_0(\omega) \\ \Theta(\omega) \end{Bmatrix} = \begin{Bmatrix} K_V(\omega)\ddot{X}_g(\omega) \\ K_{MV}(\omega)\ddot{X}_g(\omega) \end{Bmatrix} \tag{7}$$

where

$$T_V(\omega) = \omega^4\mathbf{\Gamma}^T\mathbf{H}(\omega)\mathbf{\Gamma} - \omega^2 m_T + K_V(\omega) \tag{8}$$

$$T_{VM}(\omega) = T_{MV}(\omega) = \omega^4\mathbf{\Gamma}^T\mathbf{H}(\omega)\mathbf{\Upsilon} - \omega^2 d_T + K_{VM}(\omega) \tag{9}$$

$$T_M(\omega) = \omega^4\mathbf{\Upsilon}^T\mathbf{H}(\omega)\mathbf{\Upsilon} - \omega^2 I_T + K_M(\omega) \tag{10}$$

$X_0(\omega)$ and $\Theta(\omega)$ can then be solved from equation (7) to yield

$$\begin{Bmatrix} X_0(\omega) \\ \Theta(\omega) \end{Bmatrix} = -\frac{\ddot{X}_g(\omega)}{\omega^2} \begin{Bmatrix} R_{X_0}(\omega) \\ R_\Theta(\omega) \end{Bmatrix} = X_g(\omega) \begin{Bmatrix} R_{X_0}(\omega) \\ R_\Theta(\omega) \end{Bmatrix} \tag{11}$$

where

$$R_{X_0}(\omega) = \frac{T_M(\omega)K_V(\omega) - T_{VM}(\omega)K_{MV}(\omega)}{T_V(\omega)T_M(\omega) - T_{VM}(\omega)T_{MV}(\omega)} \tag{12}$$

$$R_\Theta(\omega) = \frac{T_V(\omega)K_{MV}(\omega) - T_{MV}(\omega)K_V(\omega)}{T_V(\omega)T_M(\omega) - T_{VM}(\omega)T_{MV}(\omega)} \tag{13}$$

It should be noted that R_{X_0} and R_Θ represent the transfer functions relating the free-field ground translation to foundation translation and rotation, respectively.

Finally, substituting equation (11) into equation (6), the structural response in the complex frequency domain can be obtained in terms of the free-field ground acceleration:

$$\mathbf{X}(\omega) = \mathbf{H}(\omega)[R_{X_0}(\omega)\mathbf{\Gamma} + R_\Theta(\omega)\mathbf{\Upsilon}]\ddot{X}_g(\omega) = \mathbf{H}(\omega)\mathbf{S}(\omega)\mathbf{\Gamma}\ddot{X}_g(\omega) \tag{14}$$

where

$$\mathbf{S}(\omega) = \text{diagonal matrix with corresponding entry, } S_j(\omega) \quad \text{for } j = 1\text{–}N$$

and

$$S_j(\omega) = \left[R_{X_0}(\omega) + \frac{\Upsilon_j}{\Gamma_j} R_\Theta(\omega)\right] \tag{15}$$

For a corresponding fixed-base system, the structural response to the ground motion easily can be shown to be

$$\mathbf{X}(\omega) = \mathbf{H}(\omega)\mathbf{\Gamma}\ddot{X}_g(\omega) \tag{16}$$

Since equations (14) and (16) are equivalent except for the appearance of $\mathbf{S}(\omega)$, it can be concluded that this matrix represents the presence of SSI effects by modifying the nodal loads in the frequency domain. Subsequently, this modification can be denoted as an SSI transfer matrix in the physical space.

2.2. SSI transfer function for external control force

Since the system considered is linear, the effects of ground motion and control forces can be analysed separately and then superimposed to study the total structural behaviour of the actively controlled SSI system. A control force vector, $\mathbf{u}$, is applied alone to the system shown in Figure 1 to derive the SSI transfer function for control force.

A structure–foundation system is defined to be externally controlled if its control device exerts control forces only to the structure and is not connected to the foundation. In this case, the control force is applied as an external force to the whole system and acts like any other external load on the building. Let $\mathbf{U}(\omega)$ be the Fourier transform of $\mathbf{u}(t)$ and define

$$\mathbf{\Delta}(\omega) = \mathbf{D}\mathbf{U}(\omega) \tag{17}$$

as the nodal control force vector in the frequency domain where $\mathbf{D}$ is the mapping matrix relating control DOFs to system DOFs.

For an externally controlled system, the three equations of motion describing the system in the frequency domain can be expressed as

$$(-\omega^2\mathbf{M} + \mathrm{i}\omega\mathbf{C} + \mathbf{K})\mathbf{X}(\omega) - \omega^2\mathbf{\Gamma}X_0(\omega) - \omega^2\mathbf{\Upsilon}\Theta(\omega) = \mathbf{\Delta}(\omega) \tag{18}$$

$$-\omega^2\mathbf{\Gamma}^{\mathrm{T}}\mathbf{X}(\omega) + [K_{\mathrm{V}}(\omega) - \omega^2 m_{\mathrm{T}}]X_0(\omega) + [K_{\mathrm{VM}}(\omega) - \omega^2 d_{\mathrm{T}}]\Theta(\omega) = \mathbf{1}^{\mathrm{T}}\mathbf{\Delta}(\omega) \tag{19}$$

$$-\omega^2\mathbf{\Upsilon}^{\mathrm{T}}\mathbf{X}(\omega) + [K_{\mathrm{MV}}(\omega) - \omega^2 d_{\mathrm{T}}]X_0(\omega) + [K_{\mathrm{M}}(\omega) - \omega^2 I_{\mathrm{T}}]\Theta(\omega) = \mathbf{h}^{\mathrm{T}}\mathbf{\Delta}(\omega) \tag{20}$$

Using equation (5), the displacement vector can be solved from equation (18) as

$$\mathbf{X}(\omega) = -\mathbf{H}(\omega)[\omega^2 X_0(\omega)\mathbf{\Gamma} + \omega^2\Theta(\omega)\mathbf{\Upsilon} + \mathbf{\Delta}] \tag{21}$$

With the similar procedures shown in the previous subsection, the foundation motions $X_0(\omega)$ and $\Theta(\omega)$ can be solved as

$$X_0(\omega) = \frac{T_{\mathrm{M}}(\omega)[\mathbf{1}^{\mathrm{T}} - \omega^2\mathbf{\Gamma}^{\mathrm{T}}\mathbf{H}(\omega)] - T_{\mathrm{VM}}(\omega)[\mathbf{h}^{\mathrm{T}} - \omega^2\mathbf{\Upsilon}^{\mathrm{T}}\mathbf{H}(\omega)]}{T_{\mathrm{V}}(\omega)T_{\mathrm{M}}(\omega) - T_{\mathrm{VM}}(\omega)T_{\mathrm{MV}}(\omega)}\mathbf{\Delta}(\omega) \tag{22}$$

$$\Theta(\omega) = \frac{T_{\mathrm{V}}(\omega)[\mathbf{h}^{\mathrm{T}} - \omega^2\mathbf{\Upsilon}^{\mathrm{T}}\mathbf{H}(\omega)] - T_{\mathrm{MV}}(\omega)[\mathbf{1}^{\mathrm{T}} - \omega^2\mathbf{\Gamma}^{\mathrm{T}}\mathbf{H}(\omega)]}{T_{\mathrm{V}}(\omega)T_{\mathrm{M}}(\omega) - T_{\mathrm{VM}}(\omega)T_{\mathrm{MV}}(\omega)}\mathbf{\Delta}(\omega) \tag{23}$$

Defining

$$\mathbf{a}_{\mathrm{E}}^{\mathrm{T}}(\omega) = \frac{T_{\mathrm{M}}(\omega)[\mathbf{1}^{\mathrm{T}} - \omega^2\mathbf{\Gamma}^{\mathrm{T}}\mathbf{H}(\omega)] - T_{\mathrm{VM}}(\omega)[\mathbf{h}^{\mathrm{T}} - \omega^2\mathbf{\Upsilon}^{\mathrm{T}}\mathbf{H}(\omega)]}{T_{\mathrm{V}}(\omega)T_{\mathrm{M}}(\omega) - T_{\mathrm{VM}}(\omega)T_{\mathrm{MV}}(\omega)} \tag{24}$$

$$\mathbf{b}_{\mathrm{E}}^{\mathrm{T}}(\omega) = \frac{T_{\mathrm{V}}(\omega)[\mathbf{h}^{\mathrm{T}} - \omega^2\mathbf{\Upsilon}^{\mathrm{T}}\mathbf{H}(\omega)] - T_{\mathrm{MV}}(\omega)[\mathbf{1}^{\mathrm{T}} - \omega^2\mathbf{\Gamma}^{\mathrm{T}}\mathbf{H}(\omega)]}{T_{\mathrm{V}}(\omega)T_{\mathrm{M}}(\omega) - T_{\mathrm{VM}}(\omega)T_{\mathrm{MV}}(\omega)} \tag{25}$$

equations (21)–(23) can be combined to solve the structural response in the frequency domain in terms of the nodal control force vector:

$$\begin{aligned}\mathbf{X}(\omega) &= -\mathbf{H}(\omega)[\omega^2\mathbf{a}_{\mathrm{E}}^{\mathrm{T}}(\omega)\mathbf{\Delta}(\omega)\mathbf{\Gamma} + \omega^2\mathbf{b}_{\mathrm{E}}^{\mathrm{T}}(\omega)\mathbf{\Delta}(\omega)\mathbf{\Upsilon} + \mathbf{\Delta}] \\ &= -\mathbf{H}(\omega)[\omega^2\mathbf{\Gamma}\mathbf{a}_{\mathrm{E}}^{\mathrm{T}}(\omega) + \omega^2\mathbf{\Upsilon}\mathbf{b}_{\mathrm{E}}^{\mathrm{T}}(\omega) + \mathbf{I}]\mathbf{\Delta}(\omega) \\ &= -\mathbf{H}(\omega)\mathbf{S}_{\mathrm{E}}(\omega)\mathbf{D}\mathbf{U}(\omega)\end{aligned} \tag{26}$$

where

$$\mathbf{S}_{\mathrm{E}}(\omega) = \omega^2 \boldsymbol{\Gamma} \mathbf{a}_{\mathrm{E}}^{\mathrm{T}}(\omega) + \omega^2 \boldsymbol{\Upsilon} \mathbf{b}_{\mathrm{E}}^{\mathrm{T}}(\omega) + \mathbf{I} \tag{27}$$

For a corresponding fixed-base system, the structural response to the control force can be shown to be

$$\mathbf{X}(\omega) = -\mathbf{H}(\omega)\mathbf{D}\mathbf{U}(\omega) \tag{28}$$

Comparing equations (26) and (28), it is obvious that $\mathbf{S}_{\mathrm{E}}(\omega)$ represents the presence of SSI effects by modifying the nodal control loads in the frequency domain and is the SSI transfer matrix for control force. In a more general sense, $\mathbf{S}_{\mathrm{E}}(\omega)$ also can be interpreted as the SSI transfer matrix for any type of external loads. Therefore, the SSI transfer matrix for ground motion, $\mathbf{S}(\omega)$, is a special case of $\mathbf{S}_{\mathrm{E}}(\omega)$ when the external load is specified to be the ground excitation. This argument can be verified by reducing $\mathbf{S}_{\mathrm{E}}(\omega)\boldsymbol{\Delta}(\omega)$ to $-\mathbf{S}(\omega)\boldsymbol{\Gamma}\ddot{X}_{\mathrm{g}}(\omega)$ when $\boldsymbol{\Delta}(\omega)$ is equal to $-\boldsymbol{\Gamma}\ddot{X}_{\mathrm{g}}(\omega)$ in the case of ground excitation,[10] which also explains why the SSI transfer function for the external control force is the same as that of ground motion in the case of SDOF systems.[4] Furthermore, it is instructive to note that $\mathbf{S}_{\mathrm{E}}(\omega)$ is a full matrix having $N \times N$ independent entries in general, whereas $\mathbf{S}(\omega)$ is a diagonal matrix having only N independent entries. This difference can be explained by noting that, in the illustration here, the input excitation, $\ddot{X}_{\mathrm{g}}(\omega)$, is represented as a single component–single support ground motion excitation (even though, in theory, earthquakes are continuous, multi-component excitations which propagate independently to different structural supports). However, in the case of general external loads, there are generally N independent excitation components, $\boldsymbol{\Delta}(\omega)$, which requires N times as many SSI modification factors.

2.3. SSI transfer function for internal control force

For an internally controlled system where the control forces are internally reacted between the superstructure and foundation, the control force is an internal force to the whole system and should be distinguished from the external forces in the equation formulation. Different configurations of the controllers can result in various structural behaviours. In this study, all the internal control forces are assumed connected to the foundation for simplicity.

Similar to the previous subsection, the SSI system shown in Figure 1 is investigated. Since the control force is internally reacted in the whole SSI system in this case, the control force term appears only in the dynamic equilibrium equation for the superstructure and not in the equilibrium equations for the structure–foundation system. Therefore, the three equations of motion describing the system in the frequency domain can be expressed as

$$(-\omega^2\mathbf{M} + \mathrm{i}\omega\mathbf{C} + \mathbf{K})\mathbf{X}(\omega) - \omega^2\boldsymbol{\Gamma}X_0(\omega) - \omega^2\boldsymbol{\Upsilon}\Theta(\omega) = \boldsymbol{\Delta}(\omega) \tag{29}$$

$$-\omega^2\boldsymbol{\Gamma}^{\mathrm{T}}\mathbf{X}(\omega) + [K_{\mathrm{V}}(\omega) - \omega^2 m_{\mathrm{T}}]X_0(\omega) + [K_{\mathrm{VM}}(\omega) - \omega^2 d_{\mathrm{T}}]\Theta(\omega) = \mathbf{0} \tag{30}$$

$$-\omega^2\boldsymbol{\Upsilon}^{\mathrm{T}}\mathbf{X}(\omega) + [K_{\mathrm{MV}}(\omega) - \omega^2 d_{\mathrm{T}}]X_0(\omega) + [K_{\mathrm{M}}(\omega) - \omega^2 I_{\mathrm{T}}]\Theta(\omega) = \mathbf{0} \tag{31}$$

Expressing the displacement vector as in equation (21) and substituting it into equations (30) and (31), the foundation motions $X_0(\omega)$ and $\Theta(\omega)$ can be solved as

$$X_0(\omega) = \frac{-T_{\mathrm{M}}(\omega)[\omega^2\boldsymbol{\Gamma}^{\mathrm{T}}\mathbf{H}(\omega)] + T_{\mathrm{VM}}(\omega)[\omega^2\boldsymbol{\Upsilon}^{\mathrm{T}}\mathbf{H}(\omega)]}{T_{\mathrm{V}}(\omega)T_{\mathrm{M}}(\omega) - T_{\mathrm{VM}}(\omega)T_{\mathrm{MV}}(\omega)}\boldsymbol{\Delta}(\omega) \tag{32}$$

$$\Theta(\omega) = \frac{-T_{\mathrm{V}}(\omega)[\omega^2\boldsymbol{\Upsilon}^{\mathrm{T}}\mathbf{H}(\omega)] + T_{\mathrm{MV}}(\omega)[\omega^2\boldsymbol{\Gamma}^{\mathrm{T}}\mathbf{H}(\omega)]}{T_{\mathrm{V}}(\omega)T_{\mathrm{M}}(\omega) - T_{\mathrm{VM}}(\omega)T_{\mathrm{MV}}(\omega)}\boldsymbol{\Delta}(\omega) \tag{33}$$

Defining

$$\mathbf{a}_{\mathrm{I}}^{\mathrm{T}}(\omega) = \frac{-T_{\mathrm{M}}(\omega)[\omega^2\boldsymbol{\Gamma}^{\mathrm{T}}\mathbf{H}(\omega)] + T_{\mathrm{VM}}(\omega)[\omega^2\boldsymbol{\Upsilon}^{\mathrm{T}}\mathbf{H}(\omega)]}{T_{\mathrm{V}}(\omega)T_{\mathrm{M}}(\omega) - T_{\mathrm{VM}}(\omega)T_{\mathrm{MV}}(\omega)} \tag{34}$$

$$\mathbf{b}_{\mathrm{I}}^{\mathrm{T}}(\omega) = \frac{-T_{\mathrm{V}}(\omega)[\omega^2\boldsymbol{\Upsilon}^{\mathrm{T}}\mathbf{H}(\omega)] + T_{\mathrm{MV}}(\omega)[\omega^2\boldsymbol{\Gamma}^{\mathrm{T}}\mathbf{H}(\omega)]}{T_{\mathrm{V}}(\omega)T_{\mathrm{M}}(\omega) - T_{\mathrm{VM}}(\omega)T_{\mathrm{MV}}(\omega)} \tag{35}$$

equations (32) and (33) together with equation (21) can be combined to solve the structural response in the frequency domain in terms of the nodal control force vector:

$$\begin{aligned}\mathbf{X}(\omega) &= -\mathbf{H}(\omega)[\omega^2\mathbf{a}_\mathrm{I}^\mathrm{T}(\omega)\mathbf{\Delta}(\omega)\mathbf{\Gamma} + \omega^2\mathbf{b}_\mathrm{I}^\mathrm{T}(\omega)\mathbf{\Delta}(\omega)\mathbf{\Upsilon} + \mathbf{\Delta}] \\ &= -\mathbf{H}(\omega)[\omega^2\mathbf{\Gamma}\mathbf{a}_\mathrm{I}^\mathrm{T}(\omega) + \omega^2\mathbf{\Upsilon}\mathbf{b}_\mathrm{I}^\mathrm{T}(\omega) + \mathbf{I}]\mathbf{\Delta}(\omega) \\ &= -\mathbf{H}(\omega)\mathbf{S}_\mathrm{I}(\omega)\mathbf{D}\mathbf{U}(\omega) \end{aligned} \tag{36}$$

where

$$\mathbf{S}_\mathrm{I}(\omega) = \omega^2\mathbf{\Gamma}\mathbf{a}_\mathrm{I}^\mathrm{T}(\omega) + \omega^2\mathbf{\Upsilon}\mathbf{b}_\mathrm{I}^\mathrm{T}(\omega) + \mathbf{I} \tag{37}$$

Comparing equation (36) for the SSI system with equation (28) for the fixed-base system, $\mathbf{S}_\mathrm{I}(\omega)$ is evidently the SSI transfer matrix for control force in the case of the internally controlled system.

Combining the results shown in equations (14), (26), and (36), the governing equation of the structural response in the frequency domain can be expressed for the controlled SSI system as

$$(-\omega^2\mathbf{M} + \mathrm{i}\omega\mathbf{C} + \mathbf{K})\mathbf{X}(\omega) = -\mathbf{S}(\omega)\mathbf{\Gamma}\ddot{X}_\mathrm{g}(\omega) + \mathbf{S}_\mathrm{U}(\omega)\mathbf{D}\mathbf{U}(\omega) \tag{38}$$

where $\mathbf{S}_\mathrm{U}(\omega)$ is the SSI transfer matrix for the control force which, can be replaced by $\mathbf{S}_\mathrm{E}(\omega)$ and $\mathbf{S}_\mathrm{I}(\omega)$ for an externally or internally controlled system, respectively. Expressing in the time domain, the equation takes the form

$$\mathbf{M}\ddot{\mathbf{x}}(t) + \mathbf{C}\dot{\mathbf{x}}(t) + \mathbf{K}\mathbf{x}(t) = -\mathbf{S}(\omega) * [\mathbf{\Gamma}\ddot{X}_\mathrm{g}(\omega)] + \mathbf{S}_\mathrm{U}(\omega) * [\mathbf{D}\mathbf{U}(\omega)] \tag{39}$$

where $*$ denotes a convolution.

2.4. Simplified method via modal analysis

From the results of the previous sections, it is seen that the SSI transfer matrices for ground motion and control force are both functions of the structure transfer function, $\mathbf{H}(\omega)$. According to equation (5), the computation of $\mathbf{H}(\omega)$ involves matrix inversion operations, which can require considerable computational effort. In structural analysis, an alternative approach based on the modal superposition method is commonly utilized to uncouple the governing equations, with the additional cost of solving a corresponding eigenvalue problem. This method is especially efficient for large-order systems. Tajimi[11] first applied the modal superposition techniques to SSI analysis and in a recent study by the authors,[9] this approach was further developed to exploit fully the advantages of modal analysis. This section shows how the modal analysis can be applied to simplify the computation of the SSI transfer functions.

Based on the assumption that the fixed-base structure possesses classical normal modes, the natural frequencies and mass-orthonormalized mode shapes satisfy the following orthogonality properties:

$$\mathbf{\Phi}^\mathrm{T}\mathbf{M}\mathbf{\Phi} = \mathbf{I}, \quad \mathbf{\Phi}^\mathrm{T}\mathbf{K}\mathbf{\Phi} = \mathrm{diag}\,[\omega_j^2], \quad \mathbf{\Phi}^\mathrm{T}\mathbf{C}\mathbf{\Phi} = \mathrm{diag}\,[2\xi_j\omega_j] \tag{40}$$

where $\mathbf{\Phi}$ is the matrix consisting of normal mode shapes, ω_j the natural frequency of jth mode, ξ_j the percentage of critical damping of jth mode and diag$[\cdot]$ denotes a diagonal matrix. Defining the modal structure transfer function as

$$\bar{\mathbf{H}}(\omega) = \mathbf{\Phi}^{-1}\mathbf{H}(\omega)\mathbf{\Phi}^{-\mathrm{T}} \tag{41}$$

it is then easy to derive from equations (5) and (40) that

$$\begin{aligned}\bar{\mathbf{H}}(\omega) &= -[-\omega^2\mathbf{\Phi}^\mathrm{T}\mathbf{M}\mathbf{\Phi} + \mathrm{i}\omega\mathbf{\Phi}^\mathrm{T}\mathbf{C}\mathbf{\Phi} + \mathbf{\Phi}^\mathrm{T}\mathbf{K}\mathbf{\Phi}]^{-1} \\ &= \mathrm{diag}\left[-\frac{1}{\omega_j^2 - \omega^2 + \mathrm{i}2\omega\xi_j\omega_j}\right] \end{aligned} \tag{42}$$

Therefore, $\bar{\mathbf{H}}(\omega)$ is a diagonal matrix and its computation is trivial given that the natural frequencies are solved from the eigenvalue problem. In addition, two modal vectors can be defined as

$$\bar{\mathbf{\Gamma}} = \mathbf{\Phi}^{\mathrm{T}}\mathbf{\Gamma} = \mathbf{\Phi}^{\mathrm{T}}\mathbf{M}\mathbf{1}, \qquad \bar{\mathbf{\Upsilon}} = \mathbf{\Phi}^{\mathrm{T}}\mathbf{\Upsilon} = \mathbf{\Phi}^{\mathrm{T}}\mathbf{M}\mathbf{h} \tag{43}$$

With equations (41) and (43), the following relationships can be established:

$$\mathbf{\Gamma}^{\mathrm{T}}\mathbf{H}(\omega)\mathbf{\Gamma} = \bar{\mathbf{\Gamma}}^{\mathrm{T}}\bar{\mathbf{H}}(\omega)\bar{\mathbf{\Gamma}} \tag{44}$$

$$\mathbf{\Gamma}^{\mathrm{T}}\mathbf{H}(\omega)\mathbf{\Upsilon} = \bar{\mathbf{\Gamma}}^{\mathrm{T}}\bar{\mathbf{H}}(\omega)\bar{\mathbf{\Upsilon}} \tag{45}$$

$$\mathbf{\Upsilon}^{\mathrm{T}}\mathbf{H}(\omega)\mathbf{\Upsilon} = \bar{\mathbf{\Upsilon}}^{\mathrm{T}}\bar{\mathbf{H}}(\omega)\bar{\mathbf{\Upsilon}} \tag{46}$$

and then used to simplify the computation for $T_{\mathrm{V}}(\omega)$, $T_{\mathrm{VM}}(\omega)$, and $T_{\mathrm{M}}(\omega)$ as shown in equations (8)–(10). Consequently, the SSI transfer function for ground motion in the physical space, $\mathbf{S}(\omega)$, can be obtained much more efficiently because no matrix inversion operations are required for the computation of $\bar{\mathbf{H}}(\omega)$.

To simplify the computation of the SSI transfer functions for control force, the following relationships can be established further:

$$\mathbf{\Gamma}^{\mathrm{T}}\mathbf{H}(\omega) = \bar{\mathbf{\Gamma}}^{\mathrm{T}}\bar{\mathbf{H}}(\omega)\mathbf{\Phi}^{\mathrm{T}} \tag{47}$$

$$\mathbf{\Upsilon}^{\mathrm{T}}\mathbf{H}(\omega) = \bar{\mathbf{\Upsilon}}^{\mathrm{T}}\bar{\mathbf{H}}(\omega)\mathbf{\Phi}^{\mathrm{T}} \tag{48}$$

and then used in equations (24), (25), (34), and (35) to calculate $\mathbf{S}_{\mathrm{E}}(\omega)$ or $\mathbf{S}_{\mathrm{I}}(\omega)$ efficiently.

Another advantage of the modal superposition method lies in the fact that the response of a linear structure to seismic loading generally is dominated by the first few lower modes of vibration. Thus, even for complicated systems, analysis via the superposition of only a few vibration modes usually produces satisfactory results. For most engineering applications, the computation cost can be further reduced by considering only the first few normal modes of the superstructure without introducing an unacceptable amount of error. The accuracy of this approximation will be shown in the numerical example.

3. EQUIVALENT FIXED-BASE MODEL

Due to the inclusion of the frequency-dependent SSI transfer functions, it is most convenient to formulate the governing control equation for an MDOF SSI system in the frequency domain, as shown in equation (38). However, as discussed by Smith *et al.*[4] for the study of SDOF systems, this frequency-domain formulation prohibits direct application of the control equations to determine the optimal control gains since the conventional optimal control problem is always analysed in the time domain. An SDOF replacement oscillator was used by Smith *et al.*[4] to approximate the whole SSI system with constant system parameters, which enables an approximate time-domain formulation of the control equation and the solution of optimal control gains. This formulation is re-examined here to evaluate its accuracy. A methodology is then proposed that utilizes simple system identification techniques for application to MDOF SSI systems. Finally, an iteration algorithm similar to that used in Wu and Smith[7] for SDOF systems is applied to determine optimal control gains.

3.1. Examination of the approximation via SDOF oscillator

The development of an equivalent SDOF oscillator for representation of an SSI system is based on the determination of modified natural frequency and damping values incorporating SSI effects into a fixed-base model.[4] In other words, the equation of motion for an SDOF SSI system:

$$\ddot{x} + 2\xi\omega_0\dot{x} + \omega_0^2 x = -S(\omega) * \ddot{X}_{\mathrm{g}}(\omega) \tag{49}$$

where x is the structural deformation, ω_0 the circular natural frequency of the fixed-base structure, ξ the percentage of critical damping of the fixed-base structure and $S(\omega)$ the SSI transfer function for the SDOF SSI system[4].

It can be approximated by

$$\ddot{\tilde{x}} + 2\tilde{\xi}\widetilde{\omega_0}\,\dot{\tilde{x}} + \widetilde{\omega}_0^2\tilde{x} = -\ddot{x}_g \tag{50}$$

where $\widetilde{\omega_0}$ is the modified natural frequency to account for SSI, $\tilde{\xi}$ the modified damping factor to account for SSI and $\tilde{x}$ the total system response of the SDOF replacement oscillator.

It also was shown that the structural deformation, $x(t)$, is related to $\tilde{x}(t)$ by

$$x(t) = \left(\frac{\widetilde{\omega_0}}{\omega_0}\right)^2 \tilde{x}(t) \tag{51}$$

Let m be the structural mass, $k = m\omega_0^2$ the structural stiffness and $c = 2m\xi\omega_0$ the damping coefficient of structure. Then, the accurate structural response of the SSI system can be solved in the frequency domain as

$$X(\omega) = \frac{-mS(\omega)}{-\omega^2 m + \mathrm{i}\omega c + k}\,\ddot{X}_g(\omega) \tag{52}$$

On the other hand, the approximate structural response using the approximation via an SDOF oscillator can be solved from equation (50) as

$$X^*(\omega) = \frac{-m}{-\omega^2\tilde{m} + \mathrm{i}\omega\tilde{c} + k}\,\ddot{X}_g(\omega) \tag{53}$$

where

$$\tilde{m} = \frac{k}{\widetilde{\omega}_0^2} \tag{54}$$

$$\tilde{c} = \frac{2\tilde{\xi}k}{\widetilde{\omega_0}} \tag{55}$$

It is clear from comparing equations (52) and (53) that the approximation of the SSI system via an SDOF oscillator essentially involves finding an equivalent fixed-base model with modified mass and damping values. However, it should be noted that, while the mass is modified for the equivalent fixed-base model, the effective exciting force due to ground motion is calculated using the original mass. Therefore, m, instead of $\tilde{m}$, appears in the numerator of equation (53).

In a general perspective, any number of modified structural parameters can be determined by using the appropriate equations in enforcing the requirement that the dynamic response of the equivalent fixed-base model be equal to the response of the original fixed-base structure. More generally, these modified parameters can be determined from the response equations (which, in number, are equal to or greater than the number of parameters) by using selected algorithms to minimize the errors in calculated responses. This concept is similar to the parametric system identification problem which attempts to determine structural parameters such as stiffness or damping based on a set of equations together with inputs (i.e. excitations) and outputs (i.e. structural responses) of a system.

The effectiveness of the equivalent fixed-base model is dependent on the choice of the modified parameters and response equations. While keeping the structural stiffness unchanged, the adopted methodology determines the modified $\tilde{m}$ and $\tilde{c}$ of the equivalent fixed-base model (or, $\tilde{\omega}_0$ and $\tilde{\xi}$ of the replacement oscillator) by matching the resonant amplitude of the spring force and the frequency at which it occurs for the actual and approximate systems. This procedure results in excellent accuracy except for a steady error in the high-frequency range.[12,13]

The excellent accuracy exhibited by the above method can be explained by examining equations (52) and (53). In the low-frequency range (i.e., $\omega \to 0$), $S(\omega) \to 1$ (i.e. no SSI effects), which results in

$$X \to -\frac{m}{k}\,\ddot{X}_g \tag{56}$$

and

$$X^* \to -\frac{m}{k}\ddot{X}_g \tag{57}$$

In addition, the spring forces and, consequently, the structural displacements for the approximate and actual systems are matched at the resonant frequency. Therefore, the approximation is expected to have excellent agreement with the actual results from the low-to-medium-frequency range (i.e., frequencies that are reasonably close to the resonance frequency). However, for higher exciting frequencies, and as $\omega \to \infty$,

$$X \to -X_g \tag{58}$$

whereas

$$X^* \to -\frac{m}{\tilde{m}}X_g \tag{59}$$

This indicates that the high-frequency response of the equivalent fixed-base model is different from that of the actual system by a factor of $m/\tilde{m}$ (or, $\tilde{\omega}_0^2/\omega_0^2$). Hence, it is expected that the accuracy of this approximation would deteriorate when the system is subjected to high-frequency excitations. For dynamic analyses of most civil engineering structures, this methodology is still effective since the frequency content of the excitation is usually in the low-to-medium range, and the contribution of high-frequency response is unimportant.

Based on the analogy developed for the previous case, an alternative method is to keep the structural mass unchanged and determine the modified damping and stiffness ($\tilde{c}$ and $\tilde{k}$) of the equivalent fixed-base model by matching the inertial force at the resonant frequency for the actual and approximate systems. In this case, the structural displacements for both the actual and approximate systems approach $-X_g$ as $\omega \to \infty$, whereas

$$X \to -\frac{m}{k}\ddot{X}_g \tag{60}$$

$$X^* \to -\frac{m}{\tilde{k}}\ddot{X}_g \tag{61}$$

as $\omega \to 0$. Therefore, this approximate model would well represent the actual system in the medium to high-frequency range, but its accuracy would deteriorate in the low-frequency range. Consequently, this alternative method typically is not suitable for dynamic analysis of civil engineering structures subjected to earthquake or other naturally occurring loadings.

3.2. Generalization to equivalent MDOF fixed-base model

As discussed in the previous subsection, the approximation via an SDOF oscillator used in Reference 4 can be interpreted as a special case of a more general methodology approximating the actual SSI system by an equivalent fixed-base model. Based on this extended concept, it is easy to generalize the methodology to obtain an accurate representation of the actual MDOF SSI system with an equivalent MDOF fixed-base model. In addition, since there are N resonant peaks for an N-DOF system, the dominant-frequency range is more extensive than in the case of an SDOF system, and the approximation is required to have good accuracy over a wider range of exciting frequencies. Therefore, the equivalent fixed-base model is determined in the frequency domain by matching the responses of a number of different frequencies. A simple system identification technique using the least-squares method is applied herein to minimize the matching error.

Similar to that for an equivalent SDOF fixed-base model, the MDOF fixed-base model, the MDOF fixed-base model is formulated to keep the stiffness matrix $\mathbf{K}$ unchanged and determine the modified mass matrix $\tilde{\mathbf{M}}$ and damping matrix $\tilde{\mathbf{C}}$ such that the dominant structural response of the actual SSI system in the low-to-medium-frequency range can be captured accurately. Expressed in the frequency domain, the

governing equation for an equivalent fixed-base model with applied control forces takes the form

$$-\omega^2\tilde{\mathbf{M}}\mathbf{X}(\omega) + \mathrm{i}\omega\tilde{\mathbf{C}}\mathbf{X}(\omega) + \mathbf{K}\mathbf{X}(\omega) = -\boldsymbol{\Gamma}\ddot{X}_{\mathrm{g}}(\omega) + \mathbf{D}\mathbf{U}(\omega) \tag{62}$$

Again, it should be emphasized that the equivalent system is not subjected to the ground motion $\ddot{x}_{\mathrm{g}}$ but to the effective exciting force vector $-\boldsymbol{\Gamma}\ddot{x}_{\mathrm{g}}$, which is based on the original mass matrix $\mathbf{M}$. Since the matrices to be determined are $\tilde{\mathbf{M}}$ and $\tilde{\mathbf{C}}$ of the equivalent model, equation (62) can be reformulated further as

$$-\omega^2\tilde{\mathbf{M}}\mathbf{X}(\omega) + \mathrm{i}\omega\tilde{\mathbf{C}}\mathbf{X}(\omega) = -\boldsymbol{\Gamma}\ddot{X}_{\mathrm{g}}(\omega) + \mathbf{D}\mathbf{U}(\omega) - \mathbf{K}\mathbf{X}(\omega) = \mathbf{F}(\omega) \tag{63}$$

where $\mathbf{F}$ is the effective load vector representing the excitation force, the restoring force, and the control force. Equation (38) then can be used to simulate the structural responses at different frequencies.

The following equation in matrix form can be used to determine $\tilde{\mathbf{M}}$ and $\tilde{\mathbf{C}}$ from equation (63):

$$\left[\begin{array}{c|c} -\omega_{(1)}^2\mathbf{X}_{(1)}^{\mathrm{T}} & -\mathrm{i}\omega_{(1)}\mathbf{X}_{(1)}^{\mathrm{T}} \\ \hline \vdots & \vdots \\ \hline -\omega_{(L)}^2\mathbf{X}_{(L)}^{\mathrm{T}} & -\mathrm{i}\omega_{(L)}\mathbf{X}_{(L)}^{\mathrm{T}} \end{array}\right] \left\{\begin{array}{c} \tilde{\mathbf{M}}^{\mathrm{T}} \\ \hline \tilde{\mathbf{C}}^{\mathrm{T}} \end{array}\right\} = \left\{\begin{array}{c} \mathbf{F}_{(1)}^{\mathrm{T}} \\ \hline \vdots \\ \hline \mathbf{F}_{(L)}^{\mathrm{T}} \end{array}\right\} \tag{64}$$

where the subscript denotes the values evaluated at different frequencies and L is the total number of chosen frequencies. It should be noted that $\tilde{\mathbf{M}}$ and $\tilde{\mathbf{C}}$ are real matrices but $\mathbf{X}$ and $\mathbf{F}$ are complex-valued. Therefore, it is convenient to separate the real and imaginary parts of equation (64) and reformulate such that

$$\left[\begin{array}{c|c} -\omega_{(1)}^2\Re\{\mathbf{X}_{(1)}^{\mathrm{T}}\} & \Re\{\mathrm{i}\omega_{(1)}\mathbf{X}_{(1)}^{\mathrm{T}}\} \\ \hline -\omega_{(1)}^2\Im\{\mathbf{X}_{(1)}^{\mathrm{T}}\} & \Im\{\mathrm{i}\omega_{(1)}\mathbf{X}_{(1)}^{\mathrm{T}}\} \\ \hline \vdots & \vdots \\ \hline -\omega_{(L)}^2\Re\{\mathbf{X}_{(L)}^{\mathrm{T}}\} & \Re\{\mathrm{i}\omega_{(L)}\mathbf{X}_{(L)}^{\mathrm{T}}\} \\ \hline -\omega_{(L)}^2\Im\{\mathbf{X}_{(L)}^{\mathrm{T}}\} & \Im\{\mathrm{i}\omega_{(L)}\mathbf{X}_{(L)}^{\mathrm{T}}\} \end{array}\right] \left\{\begin{array}{c} \tilde{\mathbf{M}}^{\mathrm{T}} \\ \hline \tilde{\mathbf{C}}^{\mathrm{T}} \end{array}\right\} = \left\{\begin{array}{c} \Re\{\mathbf{F}_{(1)}^{\mathrm{T}}\} \\ \hline \Im\{\mathbf{F}_{(1)}^{\mathrm{T}}\} \\ \hline \vdots \\ \hline \Re\{\mathbf{F}_{(L)}^{\mathrm{T}}\} \\ \hline \Im\{\mathbf{F}_{(L)}^{\mathrm{T}}\} \end{array}\right\} \tag{65}$$

where $\Re$ and $\Im$ denote the real and imaginary parts of a complex-valued quantity, respectively. In equation (65), there are $2L \times N$ equations to solve for $2N \times N$ entries in $\tilde{\mathbf{M}}$ and $\tilde{\mathbf{C}}$. Accordingly, the condition of $L \geqslant N$ needs to be satisfied to have a unique or regressive solution for $\tilde{\mathbf{M}}$ and $\tilde{\mathbf{C}}$. In this study, the least-squares method is used to minimize the matching error in the case of $L > N$.

4. ITERATION ALGORITHM FOR OPTIMAL CONTROL GAINS

Once the modified mass matrix $\tilde{\mathbf{M}}$ and damping matrix $\tilde{\mathbf{C}}$ for the equivalent fixed-base model is identified from the simulated structural responses of equation (38), the time-domain version of equation (62) can be used to determine the control gains by solving the algebraic Riccati equation. However, it should be recalled that equation (62) is established based on given control forces (control gains). Therefore, the determination of optimal control gains requires the use of an iterative technique.

Similar to what is used in Wu and Smith[6,7] for SDOF systems, an iteration algorithm is established, as shown in Figure 2, to solve for the control gains of an MDOF SSI system. To start the iteration algorithm, $\mathbf{S}(\omega)$ and $\mathbf{S}_{\mathrm{U}}(\omega)$ are first assumed to be identity matrices, corresponding to a fixed-base system, and then the

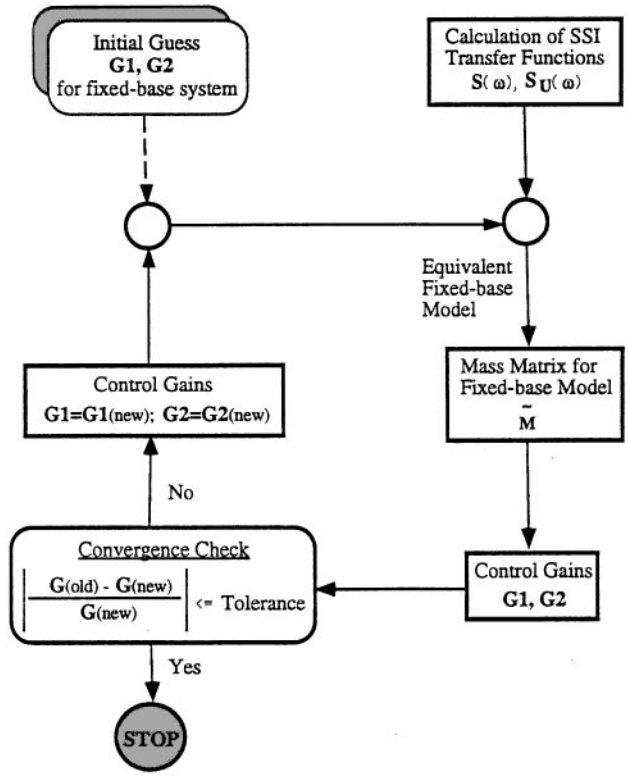

Figure 2. Iterative algorithm for controlled MDOF SSI systems

iterative procedure continues until the control gains converge to the values within certain tolerances. In contrast to the iteration for an SDOF system,[6,7] the control gains associated with structural displacements are not constant during the iteration process, as illustrated in the following numerical example.

It should be recalled that equation (62) is an approximation to the exact governing equation of motion for the controlled SSI system given by equation (38). Therefore, once the gain factors are obtained in the simulation, they are substituted into equation (38) to determine accurately the structural deformation and velocity needed in evaluating the corresponding control forces and performance indices.

5. NUMERICAL EXAMPLE

A five-storey shear building resting on a homogeneous elastic soil through a rigid square foundation is considered to demonstrate the proposed methodology. Table I summarizes all the parameters for the structural model, foundation and soil. A uniform modal damping is chosen to be 2 percent of the critical damping for each mode. It is assumed that the external control forces are applied to reduce the structural response. Two different soil stiffnesses, represented through variations in the shear velocity, v_s, are chosen to illustrate varying degrees of SSI effects.

5.1. Computation of SSI transfer functions

As a first step, the computation of SSI transfer functions is conducted. The direct formulation in the physical space and an alternative formulation in the modal space are both applied to calculate the SSI

Table I. System parameters for MDOF numerical example

Model	Parameter	Symbol	Value	Unit
Structure	Floor mass	$m_j, j = 1–5$	60,000	kg
	Column stiffness	$k_j, j = 1–5$	60,000	kN/m
	Foundation-to-storey height	$h_j, j = 1–5$	$5 \times j$	m
	Floor moment of inertia	$I_j, j = 1–5$	240,000	kg/m^2
Foundation	Half-side length	b	5	m
	Mass	m_0	120,000	kg
	Moment of inertia	I_0	240,000	kg/m^{-2}
Soil	Mass density	ρ	1,700	kg/m^3
	Poisson's ratio	ν	1/3	·
	Shear velocity	v_s	300	
			100	m/s

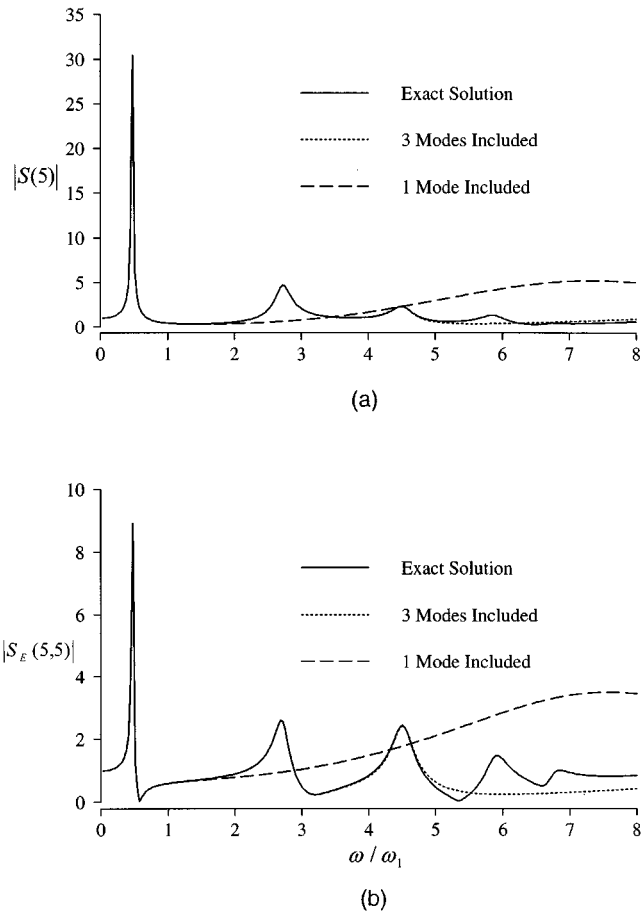

Figure 3. SSI transfer function for ground motion and external control force: (a) ground motion; (b) external control force

transfer functions for ground motion and control force, utilizing the complex foundation impedance functions investigated by Wong and Luco.[14] Coupling impedances also are included in the computation.

To show the accuracy of the formulation in the modal space, some elements in the SSI transfer matrices for ground motion and control force are selected to compare with the results obtained from the direct formulation in the physical space. For the ground motion, the magnitude of the SSI transfer factor corresponding to the fifth floor, $|S(5)|$, is plotted in Figure 3(a). For the control force, Figure 3(b) illustrates the magnitude of the (5, 5) element in the SSI transfer function, $|S_E(5, 5)|$. When all the five vibrational modes of the structure are considered in the modal formulation, the solutions are exactly the same as those from the direct formulation.

Two other sets of solutions considering only the first and the first three normal modes also are plotted in Figure 3, respectively. It is observed that the solution which includes three modes shows excellent agreement with the exact solution except for a slight difference noted in the high-frequency range. Even with use of the first mode alone, the accuracy is good up through a frequency range equal to twice the fundamental resonant frequency. The computational efficiency for these two formulations is compared in Table II, where the total flops (floating-point operations per second) required to obtain the SSI transfer functions at 100 frequencies are shown for the program run using MATLAB. All analyses were performed on a SUN-Sparcstation. It is found that the computational cost with the modal formulation is only 28 per cent of that using the direct formulation to obtain $\mathbf{S}(\omega)$ in this example. As for the calculation of $S_E(\omega)$, the modal formulation can save 51 per cent of computation time. When the approximation using only a few modes of vibration is employed, the computation cost can be further reduced.

Comparing the formulations in equations (27) and (37), it is clear that for internally controlled systems, the calculation of the SSI transfer function for the control force is similar to that for externally controlled systems with a negligible difference in computation time. Therefore, the trends observed in this example for an externally controlled system can be extended to the internally controlled system.

Table II. Comparison of flops for physical and modal space analyses

SSI transfer functions	Flops for physical space analysis (K)	Flops for modal analysis (K)		
		All modes	3 modes	1 mode
$\mathbf{S}(\omega)$	317	89	76	62
$\mathbf{S}_E(\omega)$	437	214	182	148

Table III. Comparison of mass and damping matrices

Model	Mass matrix (10^3 kg)	Damping matrix (10^3 kg/s)
Fixed-base structure	$\begin{bmatrix} 60 & 0 & 0 & 0 & 0 \\ 0 & 60 & 0 & 0 & 0 \\ 0 & 0 & 60 & 0 & 0 \\ 0 & 0 & 0 & 60 & 0 \\ 0 & 0 & 0 & 0 & 60 \end{bmatrix}$	$\begin{bmatrix} 103{\cdot}0 & -30{\cdot}0 & -5{\cdot}1 & -2{\cdot}0 & -1{\cdot}3 \\ -30{\cdot}0 & 98{\cdot}0 & -32{\cdot}0 & -6{\cdot}4 & -3{\cdot}3 \\ -5{\cdot}1 & -32{\cdot}0 & 96{\cdot}7 & -33{\cdot}0 & -8{\cdot}4 \\ -2{\cdot}0 & -6{\cdot}4 & -33{\cdot}0 & 94{\cdot}6 & -38{\cdot}0 \\ -1{\cdot}3 & -3{\cdot}3 & -8{\cdot}4 & -38{\cdot}0 & 65{\cdot}1 \end{bmatrix}$
Equivalent structure	$\begin{bmatrix} 61{\cdot}5 & -0{\cdot}6 & 0{\cdot}02 & -0{\cdot}3 & 5{\cdot}9 \\ 2{\cdot}40 & 58{\cdot}8 & 0{\cdot}42 & -0{\cdot}9 & 11{\cdot}9 \\ 3{\cdot}28 & -1{\cdot}8 & 60{\cdot}8 & -1{\cdot}5 & 17{\cdot}9 \\ 4{\cdot}16 & -2{\cdot}5 & 1{\cdot}21 & 57{\cdot}9 & 23{\cdot}9 \\ 5{\cdot}04 & -3{\cdot}1 & 1{\cdot}60 & -2{\cdot}7 & 89{\cdot}9 \end{bmatrix}$	$\begin{bmatrix} -37{\cdot}0 & 139{\cdot}0 & -134 & 70{\cdot}1 & -24{\cdot}0 \\ -188 & 291{\cdot}0 & -180 & 71{\cdot}3 & -26{\cdot}0 \\ -183 & 186{\cdot}0 & -71{\cdot}0 & 50{\cdot}3 & -31{\cdot}0 \\ -199 & 136{\cdot}0 & -220 & 183{\cdot}0 & -60{\cdot}0 \\ -217 & 263{\cdot}0 & -214 & 56{\cdot}2 & 42{\cdot}6 \end{bmatrix}$

5.2. Accuracy of equivalent fixed-base model

To evaluate the accuracy of an equivalent MDOF fixed-base model in representing the actual system, the aforementioned SSI system without the application of control forces is investigated. In this case, $N = 5$ and the simulation frequencies are uniformly chosen over the frequency domain from $\omega = 0$ to $\omega = 8\omega_1$ (eight times of the fundamental frequency) with a total number of $L = 1000$, which covers all the five resonant peaks. Equation (65) is used to identify the equivalent fixed-base model. The mass and damping matrices for the equivalent model together with those of the original superstructure are listed in Table III.

The amplitudes of the structural responses for the bottom, third, and roof floors are plotted in Figures 4–6 for (1) the actual SSI system and (2) the equivalent fixed-base model with modified mass and damping matrices. The response amplitude is normalized with respect to the amplitude of the ground motion, and the exciting frequency is normalized with respect to the fundamental frequency. Comparison of these results shows that the equivalent model represents the actual SSI system with excellent accuracy. As expected, this approximation is almost perfect in the low-frequency range, which covers the first few dominant modes of the SSI system. Even though the differences in the vicinity of the sharp peak at the fundamental frequency are obscure in the figures, the numerical values are checked to be of good accuracy. In the high-frequency range

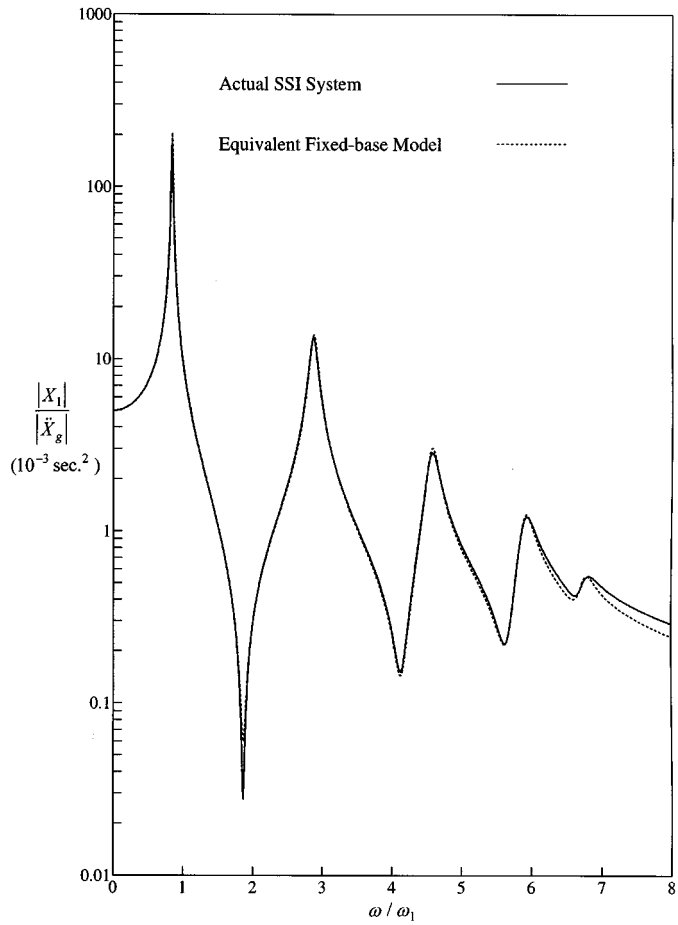

Figure 4. Structural response for the bottom floor

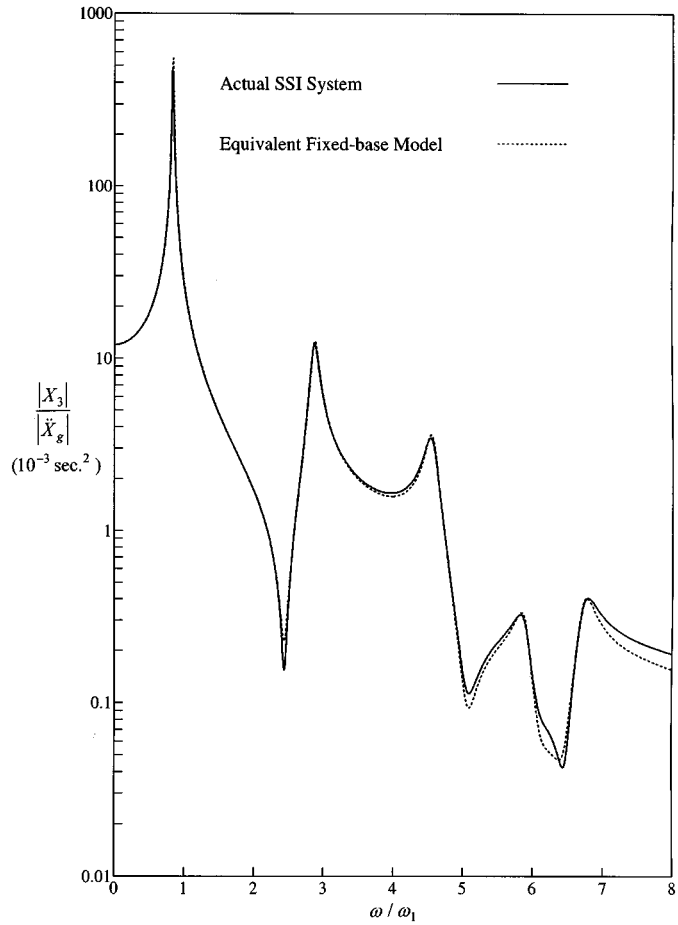

Figure 5. Structural response for the third floor

where the contribution to the total structural response is usually insignificant, the accuracy has deteriorated but the approximate responses are still representative of the actual system.

5.3. Comparison of control algorithms

Optimal control algorithms are based on the minimization of a quadratic performance index whose objective is to maintain the desired system state while minimizing the control effort. For a linear system, this performance index can be defined as

$$J = \int_0^{t_f} [\mathbf{z}^T \mathbf{Q} \mathbf{z} + \mathbf{u}^T \mathbf{R} \mathbf{u}]\, dt \tag{66}$$

where $\mathbf{z}^T$ is the state vector $= [\mathbf{x}^T | \dot{\mathbf{x}}^T]$, $\mathbf{u}$ the vector of control forces, $\mathbf{Q}$ the weighting matrix for the structural response, $\mathbf{R}$ the weighting matrix for the control force and t_f duration of the excitation.

To study the effectiveness of the control algorithm considering SSI effects versus that which uses a simple fixed-base model to determine the optimal control gains, an external control force is assumed to be applied on the roof of the structure. This results in

$$\mathbf{D} = \{0\ 0\ 0\ 0\ 1\}^T$$

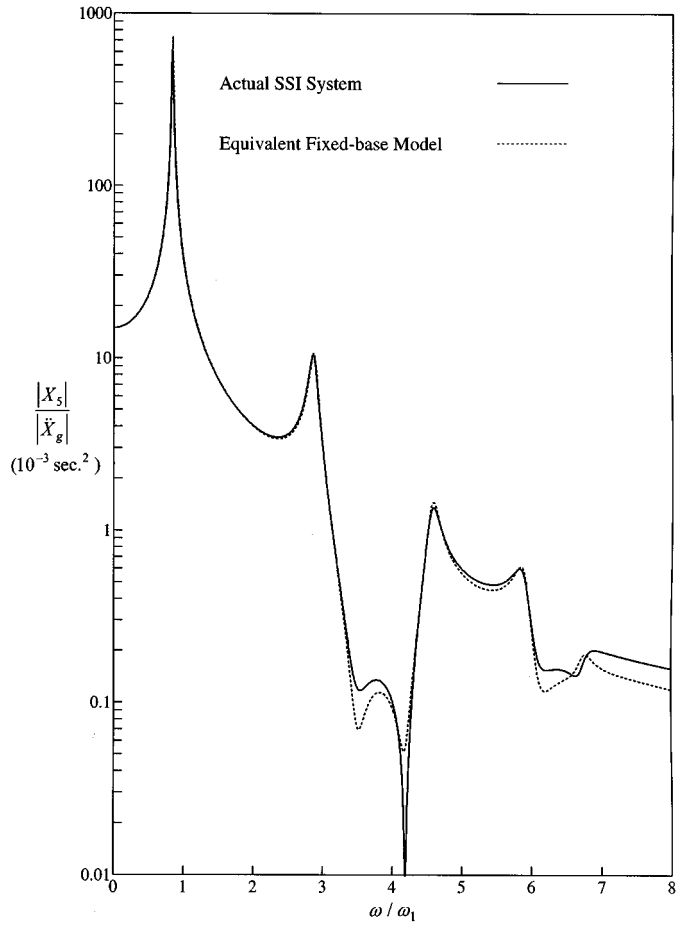

Figure 6. Structural response for the top floor

and $\mathbf{u} = u$, a single control force. For brevity of description, the latter algorithm, which assumes a fixed-base model, is referred to as the first approach. The former algorithm which considers the total SSI system is referred to as the second approach. In addition, for simplicity, the weighting matrices for the quadratic performance index are chosen as

$$\mathbf{Q} = \left[\begin{array}{c|c} \mathbf{K} & \mathbf{0} \\ \hline \mathbf{0} & \mathbf{0} \end{array}\right], \qquad \mathbf{R} = \beta \mathbf{I}_5$$

where $\mathbf{I}_5$ is a 5×5 identity matrix and the coefficient β determines the relative importance of minimizing control energy versus maximizing control effectiveness. Larger values of β indicate that minimization of control energy is considered more important, whereas smaller values of β refer to an increased importance of control effectiveness.[15]

For illustration, the 1989 Loma Prieta earthquake is chosen as the free-field ground motion. Its accelerogram, shown in Figure 7, shows a peak acceleration of 0·4g. All the analyses are first performed in the frequency domain and then the time histories of the desired quantities are determined using inverse Fourier transform. Two types of soils (stiff: $v_s = 300$ m/s and soft: $v_s = 100$ m/s) are considered in this numerical example to compare the control effectiveness of the two control approaches with and without SSI effects. In addition, two different values of the coefficient β (10^{-6}–10^{-7}) are chosen to demonstrate varying degrees of

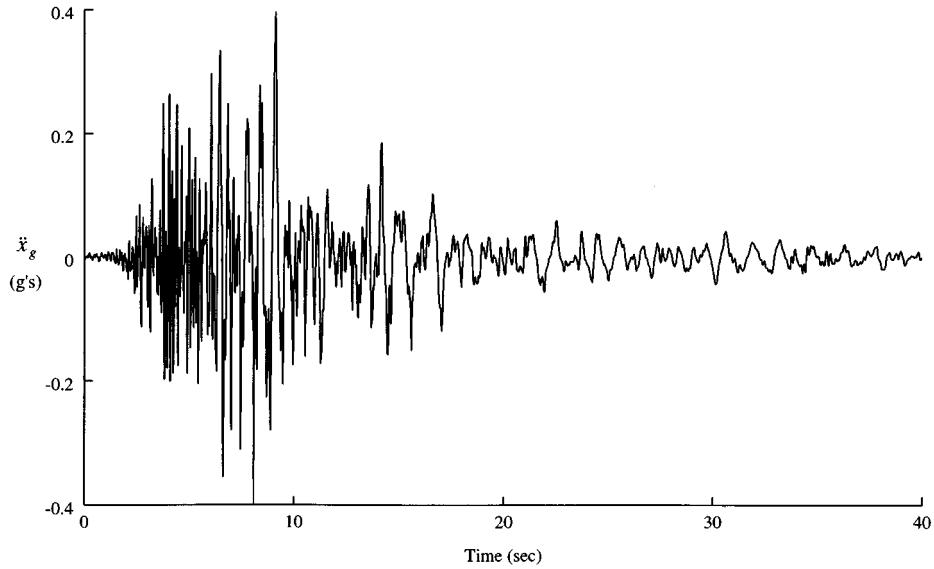

Figure 7. Acceleration time history, horizontal ground motion (filtered) from Capitola Station, Loma Prieta Earthquake, 1989

Table IV. Comparison of optimal control gains

System parameters		Control gains without SSI	Control gains with SSI
β	v_s (m/s)	$\mathbf{G}_1/\mathbf{G}_2$ ($\times 10^5$)	$\mathbf{G}_1/\mathbf{G}_2$ ($\times 10^5$)
10^{-6}	300	$\begin{bmatrix} 0{\cdot}17 & 0{\cdot}44 & 1{\cdot}32 & 4{\cdot}67 & -9{\cdot}6 \\ -0{\cdot}0 & -0{\cdot}1 & -0{\cdot}2 & -0{\cdot}5 & -2{\cdot}9 \end{bmatrix}$	$\begin{bmatrix} -0{\cdot}1 & 0{\cdot}74 & 1{\cdot}35 & 5{\cdot}07 & -10{\cdot}0 \\ -0{\cdot}3 & -0{\cdot}29 & -0{\cdot}2 & -0{\cdot}0 & -4{\cdot}1 \end{bmatrix}$
	100	$\begin{bmatrix} 0{\cdot}17 & 0{\cdot}44 & 1{\cdot}32 & 4{\cdot}67 & -9{\cdot}6 \\ -0{\cdot}0 & -0{\cdot}1 & -0{\cdot}2 & -0{\cdot}5 & -2{\cdot}9 \end{bmatrix}$	$\begin{bmatrix} -0{\cdot}4 & 0{\cdot}0 & 2{\cdot}5 & 5{\cdot}4 & -11{\cdot}0 \\ -1{\cdot}6 & 1{\cdot}02 & -0{\cdot}1 & 1{\cdot}58 & -8{\cdot}3 \end{bmatrix}$
10^{-7}	300	$\begin{bmatrix} -0{\cdot}8 & 6{\cdot}94 & -16{\cdot}0 & 118{\cdot}0 & -130 \\ -0{\cdot}0 & -0{\cdot}00 & -0{\cdot}4 & 0{\cdot}30 & -12{\cdot}0 \end{bmatrix}$	$\begin{bmatrix} -5{\cdot}5 & 9{\cdot}86 & -16{\cdot}0 & 120{\cdot}0 & -132 \\ -1{\cdot}4 & 1{\cdot}85 & -0{\cdot}7 & 2{\cdot}56 & -16{\cdot}0 \end{bmatrix}$
	100	$\begin{bmatrix} -0{\cdot}8 & 6{\cdot}94 & -16{\cdot}0 & 118{\cdot}0 & -130 \\ -0{\cdot}0 & 0{\cdot}00 & -0{\cdot}4 & 0{\cdot}30 & -12{\cdot}0 \end{bmatrix}$	$\begin{bmatrix} -16{\cdot}0 & 3{\cdot}72 & -14{\cdot}0 & 118{\cdot}0 & -127 \\ -6{\cdot}4 & 3{\cdot}63 & -0{\cdot}5 & 9{\cdot}69 & -35{\cdot}0 \end{bmatrix}$

control effort. Therefore, a total of four sets of results representing the different soils and control efforts is obtained for this example. Table IV lists the optimal control gains associated with the superstructure and with the SSI system for all the four cases used in the first and second approaches.

In parts (a) of Figures 8–11, the time history of the translation of the roof floor is plotted. It is seen that the second approach generally results in a greater reduction of the structural response than the first approach.

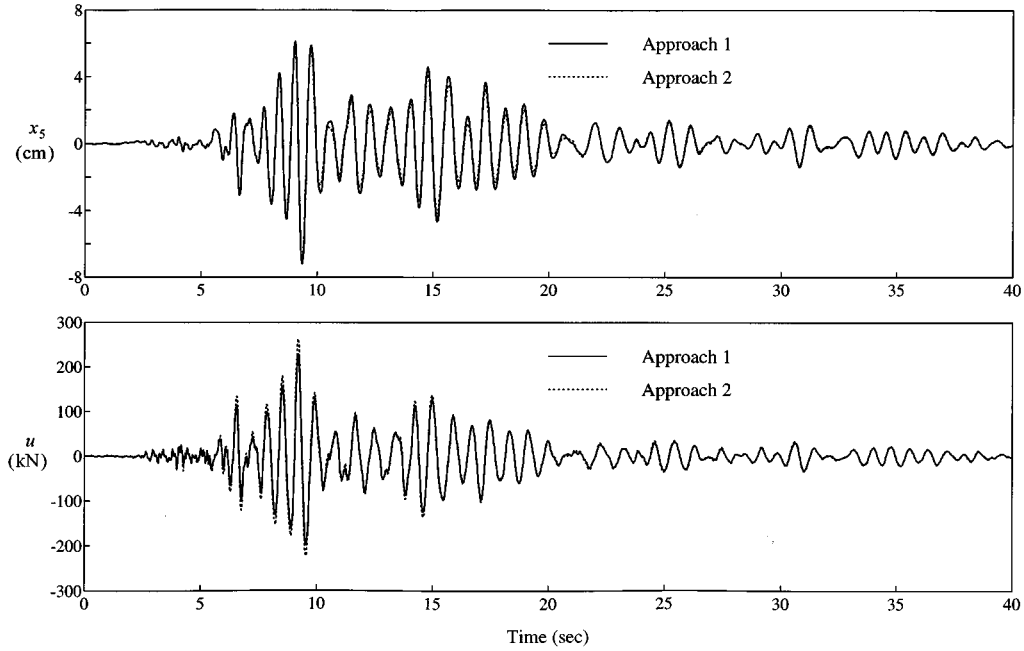

Figure 8. Comparison of response and control force ($v_s = 300$ m/s, $\beta = 10^{-6}$)

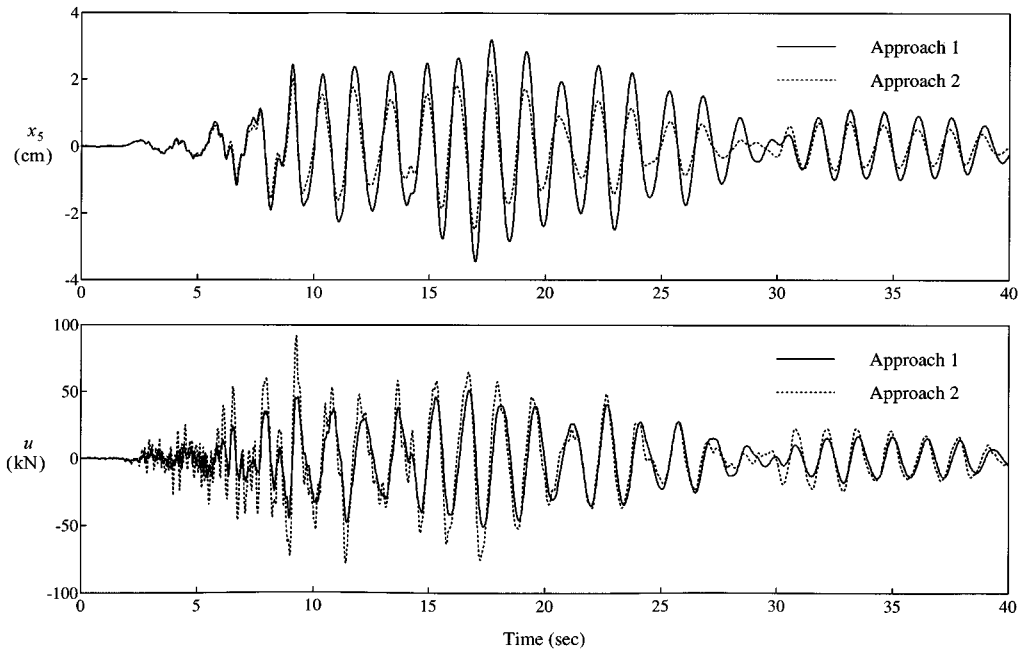

Figure 9. Comparison of response and control force ($v_s = 100$ m/s, $\beta = 10^{-6}$)

This indicates that the second approach predicts a higher degree of control effectiveness from the standpoint of reducing the structural response. It should also be noted that the difference between these two approaches is more significant for the soft soil. In parts (b) of Figures 8–11, the time histories of the control force are

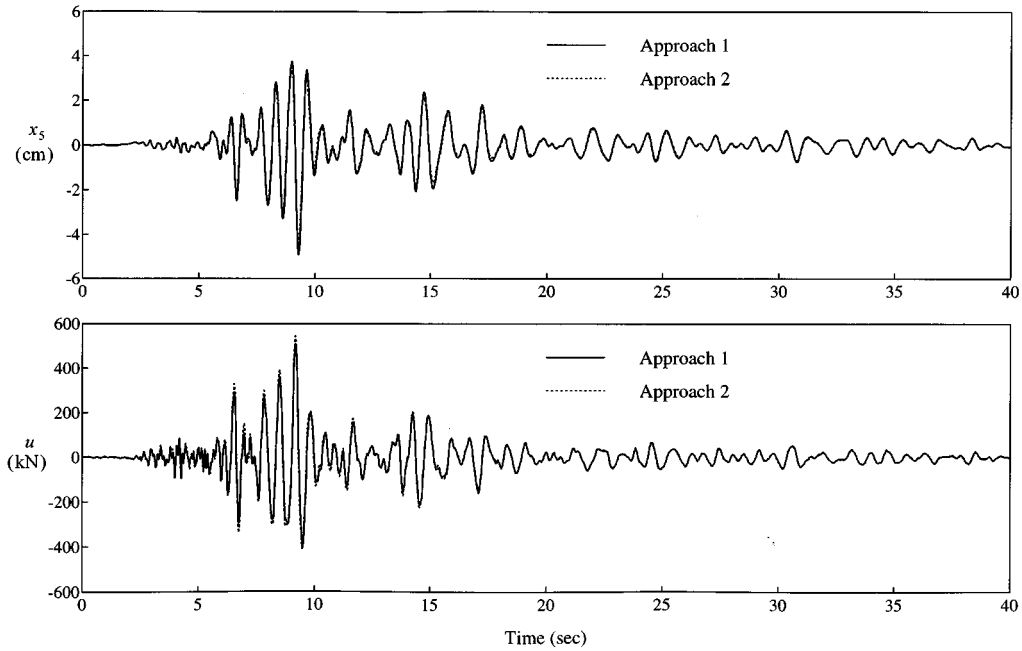

Figure 10. Comparison of response and control force ($v_s = 300$ m/s, $\beta = 10^{-7}$)

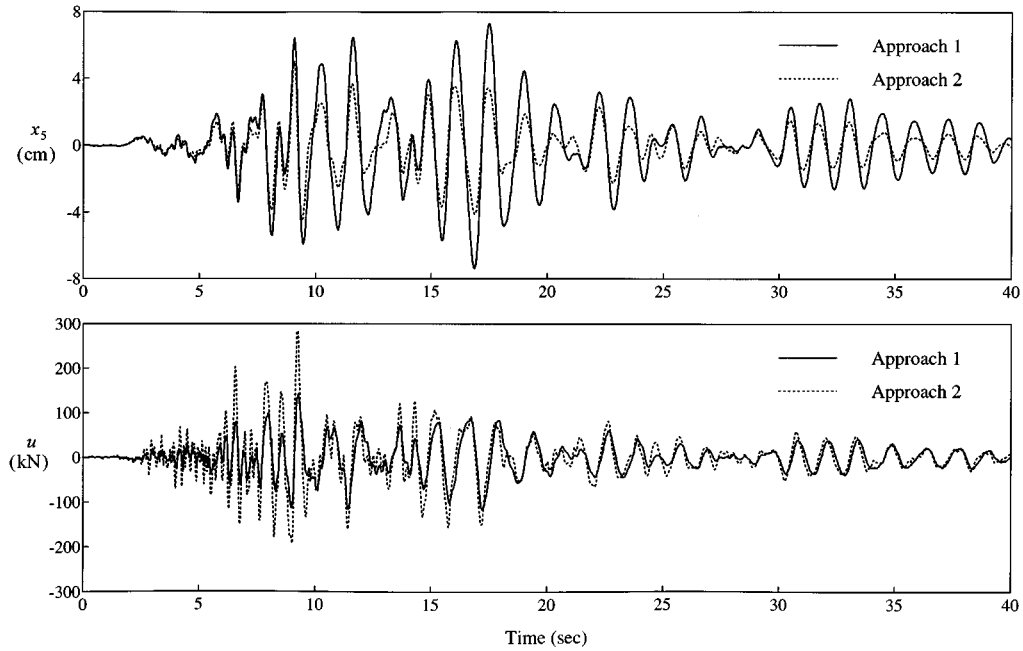

Figure 11. Comparison of response and control force ($v_s = 100$ m/s, $\beta = 10^{-7}$)

compared. It is observed that the first approach generally requires less control force than the second approach, which is not surprising considering that the first approach predicts a lesser reduction on structural response.

Table V. Comparison of performance index

System parameters		Performance index		Difference
		(Approach 1)	(Approach 2)	
β	v_s (m/s)	J_1 (10^4 J/s)	J_2 (10^4 J/s)	$(J_1 - J_2)/J_2$ (%)
10^{-6}	300	18·189	17·597	3·36
	100	9·4182	5·7637	63·41
10^{-7}	300	6·2641	6·0382	3·74
	100	2·6479	1·9645	34·79

Since the ultimate goal of the optimal control problem is to minimize the quadratic performance index J which gives an optimal balance between the desired system state and the control effort, the computation of J is necessary to assess control effectiveness completely. With the time histories of the structural responses and the control forces shown in Figures 8–11, the performance index for all the four cases is computed and listed in Table V. It is obvious that the second approach, which includes the SSI effects in determining the optimal control gains, gives the desired lower values for the performance index and is accordingly more effective in all four cases. More specifically, the advantage of using the second approach over the first is more evident for the system with soft soils, where the SSI effects are more significant. These results validate the importance of considering soil–structure interaction in an optimal structural control algorithm and the effectiveness of the proposed algorithm.

6. CONCLUSIONS

An optimal control algorithm considering soil–structure interaction effects is developed in this paper for the application to a general MDOF SSI system. This algorithm requires the integration of the following tasks:

1. Derivation of the SSI transfer functions for ground motion and control force to reduce the computational effort in calculating structural responses of SSI systems.
2. Determination of an equivalent MDOF fixed-base model to represent the actual SSI system in formulating the governing equation of motion.
3. Application of an iteration algorithm to solve the optimal control gains for the SSI system.

Some important conclusions can be drawn from the results of these work. In contrast to the case of an SDOF system, where the SSI transfer function for the external control force is the same as that for ground motion,[4] it is found that the corresponding functions for both the external and internal control forces of an MDOF system are different from that of the ground motion. In addition, an equivalent MDOF fixed-base model, with modified mass and damping matrices and the same stiffness matrix as that of the superstructure, is shown to adequately approximate the actual SSI system with excellent accuracy.

An illustrative example of a five-storey building resting on an elastic half-space is used to investigate the effectiveness of the developed control algorithm. It is shown that the control algorithm considering SSI effects is more effective in suppressing the structural response but requires more control force when compared to the corresponding results for a control algorithm assuming a fixed-base system. A further inspection reveals that the former approach always gives smaller values of the performance index, which validates the effectiveness of the control algorithm including SSI effects. The advantage of applying this algorithm also is observed to be more significant in the case of soft soils where soil–structure interaction effects are more dominant.

REFERENCES

1. H. L. Wong and J. E. Luco, 'Structural control including soil–structure interaction effects', *J. eng. mech. div. ASCE* **117**, 2237–2250 (1991).
2. T. Sato and K. Toki, 'Predictive control of seismic response of structure taking into account the soil–structure interaction', *Proc. 1st European conf. on smart structures and materials*, Glasgow, Scotland, 1992, pp. 245–250.
3. S. Alam and S. Baba, 'Robust active optimal control scheme including soil–structure interaction', *J. struct. eng. div. ASCE* **119**, 2533–2551 (1993).
4. H. A. Smith, W. H. Wu and R. I. Borja, 'Structural control considering soil-structure interaction effects', *Earthquake eng. struct. dyn.* **23**, 609–626 (1994).
5. H. A. Smith, W. H. Wu and R. I. Borja, 'Active structural control with soil–structure interaction effects', *Proc. U.S.–Italy–Japan workshop/symposium on structural control and intelligent systems*, Sorrento, Italy, 1992, pp. 204–218.
6. W. H. Wu and H. A. Smith, 'Soil–structure interaction effects for internally controlled systems', *Proc. 1993 ASME winter annual meeting*, New Orleans, LA, U.S., 1993, pp. 371–379.
7. W. H. Wu and H. A. Smith, 'Comparison of SSI effects for externally and internally controlled systems', *Smart materials struct.* **4**, 158–168 (1995).
8. A. M. Prasad, 'Studies of soil–structure and fluid–structure interaction', Ph.D. Thesis Rice University, Houston, TX, Chaps. 2 and 3, 1989, pp. 11–69.
9. W. H. Wu and H. A. Smith, 'Efficient modal analysis of structures with soil–structure interaction effects', *Earthquake eng. struct. dyn.* **24**, 283–299 (1995).
10. W. H. Wu and H. A. Smith, 'Optimal structural control considering soil–structure interaction effects', *Report No. JABEEC 112*, John A. Blume Earthquake Engineering Center, Stanford University, CA, 1994.
11. H. Tajimi, 'Discussion: building–foundation interaction effects', *J. eng. mech. eng. div. ASCE* **93**, 294–298 (1967).
12. A. S. Veletsos and J. W. Meek, 'Dynamic behavior of building-foundation systems', *Earthquake eng. struct. dyn.* **3**, 121–138 (1974).
13. A. S. Veletsos, 'Dynamics of structure-foundation systems', in W. J. Hall (ed.), *Structural and Geotechnical Mechanics*, Prentice-Hall, Englewood Cliffs, NJ, 1977, pp. 333–361.
14. H. L. Wong and J. E. Luco, 'Impedance functions for rectangular foundations on a viscoelastic half space', *J. geotech. eng. div. ASCE*, in press.
15. T. T. Soong, *Active Structural Control: Theory and Practice*, Longman Scientific & Technical, U.K., 1990.

